

Subcooled flow boiling of R-134a in vertical channels of small diameter

Claudi Martín-Callizo *, Björn Palm, Wahib Owhaib

Division of Applied Thermodynamics and Refrigeration, Department of Energy Technology, Royal Institute of Technology, KTH, 100 44 Stockholm, Sweden

Received 14 November 2005; received in revised form 4 February 2007

Abstract

Subcooled flow boiling heat transfer for refrigerant R-134a in vertical cylindrical tubes with 0.83, 1.22 and 1.70 mm internal diameter was experimentally investigated. The effects of the heat flux, $q'' = 1\text{--}26 \text{ kW/m}^2$, mass flux, $G = 300\text{--}700 \text{ kg/m}^2 \text{ s}$, inlet subcooling, $\Delta T_{\text{sub},i} = 5\text{--}15 \text{ }^\circ\text{C}$, system pressure, $P = 7.70\text{--}10.17 \text{ bar}$, and channel diameter, D , on the subcooled boiling heat transfer were explored in detail. The results are presented in the form of boiling curves and heat transfer coefficients. The boiling curves evidenced the existence of hysteresis when increasing the heat flux until the onset of nucleate boiling, ONB. The wall superheat at ONB was found to be essentially higher than that predicted with correlations for larger tubes. An increase of the mass flux leads, for early subcooled boiling, to an increase in the heat transfer coefficient. However, for fully developed subcooled boiling, increases of the mass flux only result in a slight improvement of the heat transfer. Higher inlet subcooling, higher system pressure and smaller channel diameter lead to better boiling heat transfer. Experimental heat transfer coefficients are compared to predictions from classical correlations available in the literature. None of them predicts the experimental data for all tested conditions.

© 2007 Elsevier Ltd. All rights reserved.

Keywords: Heat transfer; R-134a; Subcooled boiling; Onset of nucleate boiling

1. Introduction

Subcooled flow boiling exists when the bulk liquid temperature remains below its saturation value but the surface is hot enough for bubbles to form. The primary formation of bubbles is known as onset of nucleate boiling, ONB. According to the classical theory (Collier and Thome, 1994; Tong and Tang, 1997) bubbles formed at the wall will condense as they move out of the developing saturation boundary layer, but the appearance of these bubbles will affect the heat transfer between the wall and the fluid. At low heat fluxes or high level of subcooling, only few nucleation sites are active and a portion of the heat is transferred by

* Corresponding author. Tel.: +46 8 7907491; fax: +46 8 204161.
E-mail address: claudi@energy.kth.se (C. Martín-Callizo).

single-phase convection between patches of bubbles. This regime is termed partial nucleate boiling. As the heat flux is increased, more nucleation sites are activated until fully developed nucleate boiling, when the surface becomes fully active for nucleation. After that, as the bulk fluid is heated the saturation boundary layer grows and will eventually cover the entire channel, and the saturated nucleate boiling region is reached.

Recently there is a worldwide interest in compact heat exchangers of the microchannel type. Microchannel heat exchangers and evaporators present several advantages, both safety and cost wise, such as reduced size, higher efficiency and low fluid inventory. Because the governing phenomena are not yet well understood, much effort is being dedicated to the study of both single and two-phase heat transfer in mini and microchannels. As a summary, according to our previous work (Owhaib and Palm, 2004) single phase heat transfer and pressure drop can be well represented by classical correlations. On the other hand, and despite the discrepancy among different authors, it appears that boiling heat transfer and two-phase flow patterns cannot be properly predicted by the existing macroscale correlations (Owhaib et al., 2004). Nonetheless, very little work and experimental data can be found on subcooled flow boiling for tubes of these small diameters.

Shah (1977) compiled experimental data on different fluids and presented a correlation to predict heat transfer coefficients in subcooled boiling. The correlation is expressed in two equations applicable in the low and high subcooling regions, respectively. Essentially, the low subcooling region corresponds to fully developed boiling and the high subcooling region corresponds to partial or local boiling. The demarcation between the regions is dependent on the ratio $\Delta T_{\text{sub}}/\Delta T_{\text{sat}}$ and the boiling number, Bo .

Gungor and Winterton (1983) modified Chen's (1966) correlation by including the dependence on the boiling number in the enhancement factor. They also suggested Cooper's correlation for pool boiling in the evaporative term. Liu and Winterton (1991) presented a new correlation with improved accuracy, based on an explicit nucleate boiling term rather than an empirical boiling number.

A comprehensive review of subcooled boiling heat transfer correlations is presented by Kandlikar (1998). In the paper, he also reviews the different regions and locations of subcooled flow boiling, and introduces a newly defined significant void flow region, where the convective effects become important due to noteworthy void fraction. Kandlikar re-examines his correlation for saturated flow boiling and proposes methodology with correlations to predict heat transfer in each region.

More recently, Yin et al. (2000) showed that the subcooled boiling heat transfer of R-134a in a horizontal annular duct was not significantly affected by the mass flux, imposed heat flux nor saturation temperature, but and increase in the subcooling resulted in much better heat transfer. From their visualization tests, only the subcooling degree showed a large effect in the bubble size. Empirical correlations for the boiling heat transfer coefficient and bubble departure diameter were proposed.

Prodanovic et al. (2002) studied the transition from partial to fully developed boiling by experimental observations of bubble behaviour during subcooled flow boiling of water in a vertical heated annulus. They report a sharp transition due to a change in the heat transfer mechanisms. Microlayer evaporation is suggested to be the governing mechanism during partial boiling while bubble agitation and microconvection becomes the leading heat transfer mode for fully developed boiling. The information is used to develop a new model.

One of the first studies on subcooled flow boiling in microchannels was that of Peng et al. (1998). They pointed out that nucleation in small channels requires larger superheats. Bubble generation and growth was said to require a minimum amount of space, the *evaporating space*. If missing, *fictitious boiling* would be induced before nucleation starts.

Baird et al.'s (2000) subcooled experiments with water in minichannels suggested that heat transfer is enhanced above the additive sum of forced convection and nucleate boiling components. This enhancement is believed to be a result of transition from laminar to turbulent flow caused by incipient nucleation. Haynes and Fletcher (2003) on the other hand, conclude that subcooled boiling heat transfer coefficient in narrow passages can be described accurately as a simple additive combination of single-phase liquid-only convective heat transfer and nucleate boiling. The observed enhancement of the single-phase heat transfer component is attributed to dissolved gas release.

The present study reports on subcooled flow boiling heat transfer for refrigerant R-134a in vertical cylindrical tubes with 0.83, 1.22 and 1.70 mm internal diameter. The effects of the imposed wall heat flux, q'' , refrigerant mass flux, G , liquid inlet subcooling, $\Delta T_{\text{sub},i}$, system pressure, P , and internal channel diameter, D , on boiling incipience and subcooled boiling heat transfer are explored in detail.

2. Experimental apparatus and data reduction

The test rig was designed and constructed as schematically illustrated in Fig. 1. In the apparatus, system pressure, heat flux, mass flux and subcooling can be adjusted independently. Circulation of the fluid is driven by a magnetic gear pump with microprocessor control, type MCP-Z standard, also used as flow meter. System pressure is adjusted by fixing the cooling water flow rate in the condenser and further set within $\pm 2\%$ by controlling the electrical heat input to a tank connected to the main loop. The liquid level in the condenser defines the system pressure. Subcooling degree at the inlet of the test section is adjusted with an electrical preheater. The circuit also includes a $7\ \mu\text{m}$ filter to prevent the flow blocking from small particles.

The test sections, also shown in Fig. 1, consists of a metal (AISI 316 stainless steel) tube with inner diameter of 0.83, 1.22 and 1.70 mm respectively, and 310 mm in length. The actual heated length, z_{hs} , is 220 mm. A glass tube of the same diameter is placed in each end of the metal tube for visualization purposes, and also to insulate the test section, both electrically and thermally, from the rest of the system. The test sections are heated using an electrical DC power supply applying a potential difference directly over the test tube itself. The direct heating ensures homogeneous heat flux over the test section.

The experimental facility is instrumented with an absolute pressure transducer (Druck, 20 bar) to measure the system pressure and a differential pressure transducer (Druck, 350 mbar) for the pressure drop across the test section. 0.1 mm diameter T-type thermocouples were installed at different locations and mounted to the surface of the test tube to measure the bulk fluid temperatures, T_{fluid} , and wall temperatures, T_w , respectively. The entire test rig is well insulated, with special attention given to the test section. All tests are performed under steady-state conditions. Thermodynamic properties for R-134a, including density, enthalpy, viscosity, and thermal conductivity, are calculated with the computer code REFPROP 6.01 developed by NIST. Experimental conditions and expected uncertainties (Kline and McClintock, 1953) are summarized in Table 1.

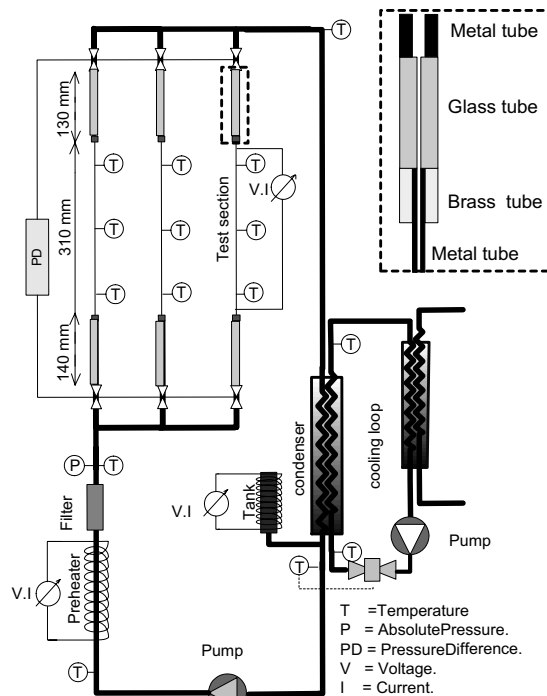


Fig. 1. Microscale heat transfer test rig and test section.

Table 1
Operating conditions and uncertainties

| Parameter | Operating range | Uncertainty |
|--|-------------------|-------------|
| D (mm) | 0.83, 1.22, 1.70 | ± 0.1 |
| P (inlet) (bar) | 7.70, 8.87, 10.17 | $\pm 0.2\%$ |
| T_{sat} ($^{\circ}\text{C}$) | 30, 35, 40 | ± 0.1 |
| G ($\text{kg}/\text{m}^2 \text{ s}$) | 300–700 | $\pm 5\%$ |
| q'' (kW/m^2) | 1–26 | $\pm 2\%$ |
| $\Delta T_{\text{sub},i}$ ($^{\circ}\text{C}$) | 5–15 | ± 0.2 |
| $T_w - T_{\text{fluid}}$ ($^{\circ}\text{C}$) | 0–25 | ± 0.1 |
| x_{th} (–) | –0.17 to 0.03 | 5% |
| h ($\text{W}/\text{m}^2 \text{ K}$) | 0–7480 | 15% |

For a given test point, the heat flux added to the test section, q'' , is calculated as

$$q'' = \frac{I \cdot V}{A}, \quad (1)$$

where V and I are, respectively, the current and voltage intensity applied to the test section, and A the heat transfer area.

Even distribution of the heat flux across the whole surface is assumed. The local heat transfer coefficient, h_z , at a certain axial position, z , is calculated from the local bulk to wall temperature difference and the heat flux as

$$h_z = \frac{q''}{T_{w,z} - T_{\text{fluid},z}}, \quad (2)$$

where $T_{w,z}$ is the calculated inside wall temperature – based on the measured outside surface temperature – at position z , $T_{\text{fluid},z}$ is the bulk fluid temperature at the same axial position – calculated from the measured inlet temperature and the heat added to the test section from the inlet to z –, and q'' is the wall heat flux to the fluid.

The thermodynamic vapour quality at any axial location, $x_{\text{th}}(z)$, is defined from the heat transferred to the fluid as

$$x_{\text{th}}(z) = \frac{q'' \pi D (z - z_{\text{sat}})}{AGi_{\text{lg}}}, \quad (3)$$

where i_{lg} is the latent heat of vaporization and z_{sat} is the position at which saturated condition would be reached (Collier and Thome, 1994) calculated as

$$z_{\text{sat}} = \frac{\dot{m}_{\text{R134a}} c_p (T_{\text{sat}} - T_i)}{q'' \pi D}, \quad (4)$$

being \dot{m}_{R134a} the refrigerant mass flow and C_p the specific heat.

3. Experimental results and discussion

In the present study, experiments on subcooled and early saturated flow boiling heat transfer were conducted with R-134a for refrigerant mass fluxes, G , ranging from 300 to 700 $\text{kg}/\text{m}^2 \text{ s}$, imposed wall heat flux, q'' , from 1 to 26 kW/m^2 , liquid inlet subcooling, $\Delta T_{\text{sub},i}$, from 5 to 15 $^{\circ}\text{C}$ and for system pressures, P , of 7.70, 8.87 and 10.17 bar (corresponding to the R-134a saturation temperatures of 30, 35 and 40 $^{\circ}\text{C}$) inside tubes of 0.83, 1.22 and 1.70 mm internal diameter. The results are presented in the form of boiling curves and heat transfer coefficients.

3.1. Boiling curves

A boiling curve plots the imposed wall heat flux versus the temperature of the heated wall. At the beginning, under subcooled liquid conditions, while increasing the heat flux between the heating surface and the liquid,

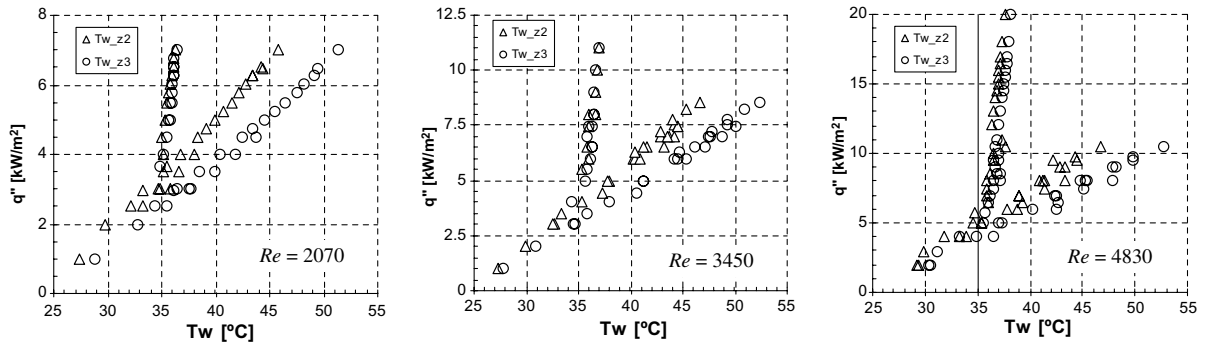


Fig. 2. Boiling curves for constant $T_{\text{sat}} = 35\text{ }^{\circ}\text{C}$, $\Delta T_{\text{sub},i} = 10\text{ }^{\circ}\text{C}$, and $G = 300, 500$ and $700\text{ kg/m}^2\text{ s}$, respectively in the 1.22 mm diameter tube at axial positions z_2 and z_3 .

the heat transfer occurs by single-phase forced convection. Liquid located close to the surface soon becomes superheated, whereas the flow core remains subcooled. Further increase in the heat flux results in increased wall superheat, ΔT_{sat} , and eventually in vapour nuclei activation. Nucleation causes the heating surface temperature to drop. The temperature undershoot at the onset of nucleate boiling, ONB, can be very large, up to $18\text{ }^{\circ}\text{C}$ for $G = 700\text{ kg/m}^2\text{ s}$ and $\Delta T_{\text{sub},i} = 10\text{ }^{\circ}\text{C}$ (see Fig. 2). As the heat flux is increased beyond ONB, more nucleation sites are activated and thus, only small increases in the wall temperature are recorded. On the other hand, when the heat flux is lowered from high values, where bubble nucleation is rather intense, nucleate boiling can be maintained until wall superheats as small as $0.3\text{ }^{\circ}\text{C}$ for $G = 300\text{ kg/m}^2\text{ s}$ and $\Delta T_{\text{sub},i} = 10\text{ }^{\circ}\text{C}$. This clearly evidences the existence of nucleation hysteresis.

Fig. 2 shows the boiling curves at two different axial positions, $z_2 = 0.41 z_{\text{hs}}$ and $z_3 = 0.93 z_{\text{hs}}$, for three different mass fluxes. Figs. 3–5 show boiling curves for $z = z_3$ and different inlet subcooling degree, channel diameter and system pressure (i.e. saturation temperature), respectively.

All experiments were performed by changing the wall heat flux, while refrigerant mass flux, inlet subcooling degree and inlet pressure were kept constant. Starting under subcooled liquid conditions, the heat flux was gradually increased until early saturation condition (low positive vapour quality) was reached at the exit of the test section. As a consequence, the scales on the y-axis of Figs. 2–5 differ. Results show that, with all other parameters being fixed, neither the mass flux nor the inlet subcooling seem to influence the maximum wall superheat or the temperature undershoot at ONB. On the other hand, both parameters affect the minimum wall superheat at which nucleation is last maintained when decreasing the heat flux. The lower the mass flux and inlet subcooling, the easier to maintain boiling, i.e. lower wall superheat is needed. The system pressure does not seem to influence the maximum wall superheat at ONB nor that to maintain nucleation. The effect of

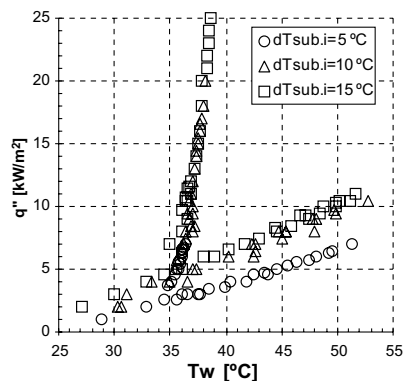


Fig. 3. Boiling curves for $D = 1.22\text{ mm}$, $T_{\text{sat}} = 35\text{ }^{\circ}\text{C}$, $G = 700\text{ kg/m}^2\text{ s}$ and $\Delta T_{\text{sub},i} = 5, 10$ and $15\text{ }^{\circ}\text{C}$, at z_3 .

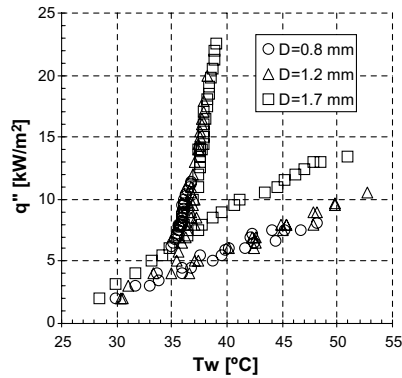


Fig. 4. Boiling curves for $T_{\text{sat}} = 35 \text{ }^\circ\text{C}$, $\Delta T_{\text{sub},i} = 10 \text{ }^\circ\text{C}$, $G = 700 \text{ kg/m}^2 \text{ s}$ and $D = 0.83, 1.22$ and 1.70 mm , at z_3 .

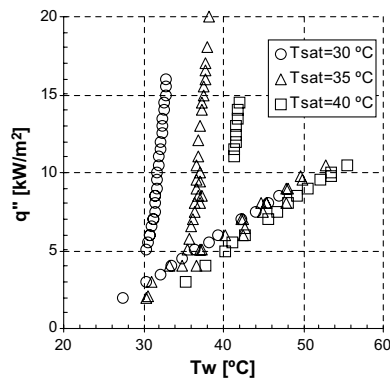


Fig. 5. Boiling curves for $D = 1.22 \text{ mm}$, $\Delta T_{\text{sub},i} = 10 \text{ }^\circ\text{C}$, $G = 700 \text{ kg/m}^2 \text{ s}$ and $T_{\text{sat}} = 30, 35$ and $40 \text{ }^\circ\text{C}$, at z_3 .

the channel diameter on the maximum wall superheat is not clear from the experiments, being larger for $D = 1.22 \text{ mm}$ ($\Delta T_{\text{sat,ONB}} = 18 \text{ }^\circ\text{C}$), than for $D = 1.70 \text{ mm}$ ($\Delta T_{\text{sat,ONB}} = 16 \text{ }^\circ\text{C}$) and $D = 0.83 \text{ mm}$ ($\Delta T_{\text{sat,ONB}} = 13 \text{ }^\circ\text{C}$) at $z = z_3$.

In the experiments the occurrence of ONB was identified both by visual observations at the outlet of the test section and temperature data. The heat flux necessary for incipience of boiling at a certain axial position z , $q''_{\text{ONB},z}$, increases with increasing mass flux, inlet subcooling, channel diameter and saturation pressure.

Experimental ONB data was compared to predictions by classical correlations by Bergels and Rohsenow (1964); and Sato and Matsumura (1964) developed for larger tube dimensions. The wall superheat needed to initiate boiling, $\Delta T_{\text{sat,ONB}}$, was found to be considerably higher for the same given values of heat and mass flux. The same trend for boiling incipience in microchannels is reported by Hapke et al. (2000); and Ghiaasiaan and Chedester (2002). This increase is related by the latter, to the gaining importance of the thermocapillary force in microchannels, which would suppress the microbubbles that tend to form on the wall cavities.

3.2. Heat transfer coefficient

The state of the subcooled liquid can be quantified in terms of the thermodynamic vapour quality, x_{th} , based on the liquid enthalpy relative to the saturation state. Defined as for saturated conditions, it results in negative values for subcooled boiling.

Effects of the mass flux on the R-134a subcooled flow boiling heat transfer coefficients at a fixed axial position, $z = z_3$, are shown in Fig. 6. For a given G , an increase in x_{th} leads to a slight decrease in the single-phase line. On the other hand, under boiling conditions, an increase in x_{th} within the subcooled region (i.e. $x_{\text{th}} < 0$) is coupled with an increase in the heat transfer coefficient.

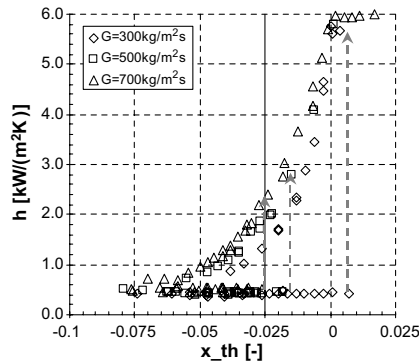


Fig. 6. Effect of the mass flux for $D = 1.22$ mm, $T_{\text{sat}} = 35$ °C and $\Delta T_{\text{sub},i} = 10$ °C, at z_3 .

In single-phase, heat transfer occurs by convection and the heat transfer coefficient, h , is essentially a function of the mass flux. Under boiling conditions, for low values of x_{th} , the heat transfer coefficient continues to show a strong dependence on G , but as x_{th} is increased, at the same time as h rises, the effect of G on h seems to gradually diminish, to become insignificant close to saturation conditions ($x_{\text{th}} \geq 0$). This could be explained by the change in mechanism governing the heat transfer. In the early, low void, subcooled boiling region the nucleate boiling contribution is small and the heat transfer coefficient is therefore strongly dependent on the mass flux. As the heat flux is further increased and more nucleation sites are activated, the contribution to heat transfer from the nucleate boiling continues to rise while the single-phase convective contribution diminishes. The local heat transfer coefficient at $z = z_3$ was found to be $h_{z_3} \approx 6$ kW/m² K for all mass fluxes, at $\Delta T_{\text{sub},i} = 10$ °C and $x_{\text{th}} \approx 0$.

With system pressure and inlet subcooling being fixed, the heat transfer coefficient in slightly subcooled flow boiling can then be determined by the vapour quality only, regardless the mass flux. Nonetheless, the vapour quality is dependent on both heat and mass flux and therefore so is the heat transfer. Heat transfer coefficient dependence on mass and heat flux can be easily appreciated in Fig. 7. For a given value of q'' , the heat transfer coefficient is clearly a function of the mass flux.

Bergels and Rohsenow (1964) suggested that bubble formation could promote bulk turbulence, thus enhancing the bulk convective contribution to total heat transfer, but Haynes and Fletcher (2003) claim that this effect is small compared to the enhancement already embodied by the nucleate boiling mechanism. This enhancement could, however, be noteworthy in the early subcooled boiling regime, where contribution from bare addition of nucleation is still quite small but turbulence promotion can be significant.

Effects of the inlet subcooling degree on the R-134a subcooled flow boiling are shown in Fig. 8. The results show that the higher the inlet subcooling degree, the higher the heat transfer coefficient for a given vapour

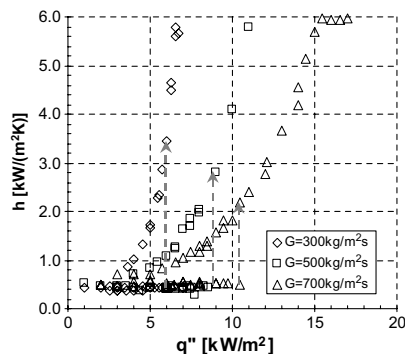


Fig. 7. Effect of the heat flux for $D = 1.22$ mm, $T_{\text{sat}} = 35$ °C, $\Delta T_{\text{sub},i} = 10$ °C and $G = 300, 500$ and 700 kg/m² s, at z_3 .

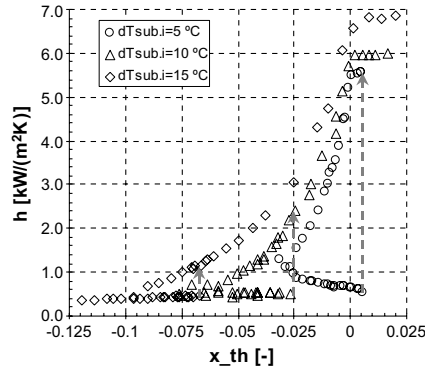


Fig. 8. Effect of the inlet subcooling degree for $D = 1.22$ mm, $T_{\text{sat}} = 35$ °C and $G = 700$ kg/m² s, at z_3 .

quality. For a higher inlet subcooling degree a higher heat flux is needed to achieve a certain vapour quality, x_{th} , at a fixed location. Under subcooled boiling conditions, the fluid close to the surface is at saturation temperature, or slightly superheated, while the fluid in the core is subcooled. With the same bulk fluid temperature (i.e. same x_{th}) and higher heat flux, the surface is more active for nucleation and the heat transfer coefficient is therefore higher.

An increase in the system pressure improves the heat transfer performance. From Fig. 9, the higher the saturation temperature, the higher the heat transfer coefficient, both for subcooled and early saturated boiling. This enhancement could be related to the activation of additional, smaller nucleation sites for higher pressures.

Fig. 10 shows the effects of the channel diameter on the heat transfer coefficient at a given axial position, $z = z_3$. From this figure, the smaller the diameter, the higher the heat transfer coefficient for a given heat flux. In all Figs. 6–10, the effect of the vapour quality on the heat transfer coefficient becomes less important in the early saturated region.

Boiling hysteresis can also be clearly seen in Figs. 6–10. From Figs. 6 and 8 it is observed that ONB is reached at higher vapour qualities the lower the mass flux and inlet subcooling. Bubbles are formed within the saturated boundary close to the heated wall, while the core remains subcooled. With the saturated boundary being big enough for the bubbles to grow and detach, the higher the inlet subcooling, the lower the core temperature and thus, the thermodynamic vapour quality. On the other hand, the higher turbulence inherent in a higher mass flux would promote bubble detachment to occur earlier. No significant changes in the thermodynamic quality at ONB could be seen due to system pressure, but a slightly lower subcooling degree (i.e. higher vapour quality) is needed to initiate boiling in a smaller tube.

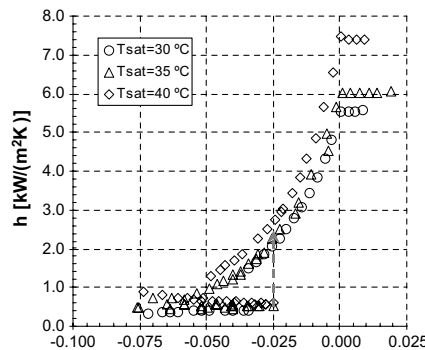


Fig. 9. Effect of the saturation pressure for $D = 1.22$ mm, $\Delta T_{\text{sub},i} = 10$ °C, and $G = 700$ kg/m² s, at z_3 .

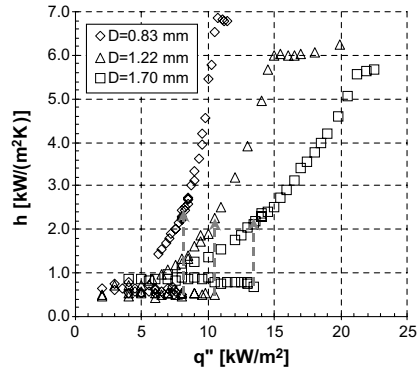


Fig. 10. Effect of the internal diameter for $T_{\text{sat}} = 35\text{ }^{\circ}\text{C}$, $\Delta T_{\text{sub},i} = 10\text{ }^{\circ}\text{C}$, and $G = 700\text{ kg/m}^2\text{ s}$, at z_3 .

Table 2
Heat transfer correlations for fully developed subcooled flow boiling

| Author(s) | Correlation formulae | Eq. | MAD (%) |
|-----------------------------|--|-----|---------|
| Shah (1977) | $q'' = (230[\dot{m} \cdot i_{\text{lg}}]^{-0.5} h_{\text{lo}} \Delta T_{\text{sat}})^2$ where h_{lo} from Dittus–Boelter $q'' = h_{\text{lo}}(T_w - T_{\text{fluid}}) + \text{Sh}_{\text{pool}}(T_w - T_{\text{sat}})$ | (5) | –19.9 |
| Gungor and Winterton (1983) | where $S = \frac{1}{1 + 1.15 \cdot 10^{-6} E^2 Re_{\text{lo}}^{1.17}}$ $E = 1 + 24,000 Bo^{1.16} + 1.37(1/\chi_{\text{tt}})^{0.86}$ h_{lo} from Dittus–Boelter h_{pool} from Cooper (1984) | (6) | +131 |
| Kandlikar (1998) | $q'' = (1058[\dot{m} \cdot i_{\text{lg}}]^{-0.7} h_{\text{lo}} \Delta T_{\text{sat}})^{1/0.3}$ where h_{lo} from Gnielinski (1976); or Pethukov and Popov (1963) | (7) | –35.2 |

3.3. Comparison to correlations

The two-phase heat transfer experimental data (201 data points) is here compared to predictions from three correlations available in the literature. Among the many correlations for subcooled flow boiling, these suggested by Shah (1977); Gungor and Winterton (1983); and Kandlikar (1998) have been chosen for this comparison. All three correlations were derived for fully developed subcooled boiling in the conventional macroscale and, to a large extent, are well accepted for these geometries. These correlations are shown in Table 2.

Many of the data points fall within a substantial error range (see Fig. 11). Being N the number of experimental data points, the mean absolute deviation, MAD, is given by

$$\text{MAD} = \frac{1}{N} \sum_{i=1}^N \left(\frac{h_{\text{pred}} - h_{\text{exp}}}{h_{\text{exp}}} \right) \cdot 100 \quad (8)$$

Shah correlation underpredicts all experimental data with a total MAD of –19.9% and does not capture the effects on the heat transfer coefficient from the different parameters. As illustrated in Table 3, the predictions show better agreement with the experimental data the larger the mass flow, the larger the inlet subcooling degree the larger the diameter, and the lower the saturation pressure. Kandlikar correlation, similar to that of Shah, underpredicts experimental data for all operating conditions (MAD = –35.2%) and that of Gungor and Winterton does not follow the trend of experimental heat transfer coefficients (MAD = +131%).

None of the correlations seem to predict well the experimental data for all tested conditions. The under prediction by Shah and Kandlikar correlations is notably higher at the early subcooled boiling region, suggesting the existence of partial subcooled boiling that would promote and early enhancement of the heat transfer coefficient.

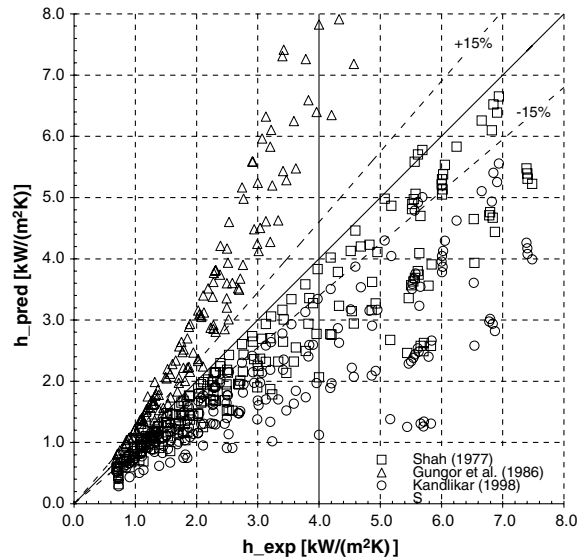


Fig. 11. Comparison of the experimental heat transfer coefficients, h_{exp} , with those predicted from correlations, h_{pred} , for all tested conditions.

Table 3

Parametric mean absolute deviation, MAD, between experiments and predictions from Shah correlation

| G (kg/m ² s) | MAD (%) | $\Delta T_{sub,i}$ (°C) | MAD (%) | D (mm) | MAD (%) | T_{sat} (°C) | MAD (%) |
|---------------------------|---------|-------------------------|---------|----------|---------|----------------|---------|
| 300 | −44.7 | 5 | −36.9 | 0.83 | −27.4 | 30 | −12.5 |
| 500 | −22.3 | 10 | −13.7 | 1.22 | −13.7 | 35 | −13.7 |
| 700 | −13.7 | 15 | −8.1 | 1.70 | −5.9 | 40 | −24.7 |

4. Conclusion

Subcooled flow boiling of R-134a in vertical tubes of 0.83, 1.22 and 1.70 mm inner diameter has been experimentally studied and results have been compared to correlations from the literature. The effects of mass flux, G , heat flux, q'' , inlet subcooling, $\Delta T_{sub,i}$, system pressure, P , and channel diameter, D , on boiling hysteresis, onset of nucleate boiling (ONB) and heat transfer coefficient have been explored in detail.

Temperature undershoot at ONB is rather significant and independent on G , $\Delta T_{sub,i}$ and P . Both G and $\Delta T_{sub,i}$ however, influence the minimum wall superheat at which boiling is last maintained; being smaller for lower G and $\Delta T_{sub,i}$. The effect of D on the maximum wall superheat is not clear from the experiments. Macroscale correlations underpredict q''_{ONB} in the experiments, where it was found to increase with increasing G , $\Delta T_{sub,i}$, P and D .

In single phase and early subcooled boiling, heat transfer coefficient, h , is strongly dependent on mass flux. For fully developed subcooled boiling, with all other parameters being fixed, the heat transfer can be determined from the thermodynamic quality only, with no dependence of G and q'' . On the other hand, given a vapour quality, the higher $\Delta T_{sub,i}$ and P , the higher h . The boiling heat transfer coefficient is also higher, close to saturation, for smaller diameter tubes. None of the macroscale correlations is in agreement with the experimental data for all tested conditions.

Acknowledgement

Work supported in part by the European Community’s Human Potential Programme under contract HPRN-CT-2002-00204 [HMTMIC].

References

- Baird, J.R., Bao, Z.Y., Fletcher, D.F., Haynes, B.S., 2000. Local flow boiling heat transfer coefficients in narrow conduits. *Multi. Sci. Technol.* 12, 129–144.
- Bergels, A.E., Rohsenow, W.M., 1964. The determination of forced-convection surface-boiling heat transfer. *ASME J. Heat Transf.* 86, 365–372.
- Chen, J.C., 1966. Correlation for boiling heat transfer to saturated fluids in convective flow. *Ind. Eng. Chem. Process Des. Develop.* 5, 322–329.
- Collier, J.G., Thome, J.R., 1994. *Convective boiling and condensation*, third ed. Oxford Science Publications, 183–213.
- Cooper, M.G., 1984. Saturated nucleate pool boiling – a simple correlation. In: 1st UK National Heat Transfer Conference, IchemE Symposium Series 86, pp. 785–793.
- Ghiaasiaan, S.M., Chedester, R.C., 2002. Boiling incipience in microchannels. *Int. J. Heat Mass Transf.* 45, 4599–4606.
- Gnielinski, V., 1976. New equations for heat transfer in turbulent pipe and channel flow. *Int. Chem. Eng.* 16, 359–368.
- Gungor, K.E., Winterton, R.H.S., 1983. A general correlation for flow boiling in tubes and annuli. *Int. J. Heat Mass Transf.* 29, 351–358.
- Hapke, I., Boye, H., Schmidt, J., 2000. Onset of nucleate boiling in minichannels. *Int. J. Therm. Sci.* 39, 505–513.
- Haynes, B.S., Fletcher, D.F., 2003. Subcooled flow boiling heat transfer in narrow passages. *Int. J. Heat Mass Transf.* 46, 3673–3682.
- Kandlikar, S.G., 1998. Heat transfer characteristics in partial boiling, fully developed boiling, and significant void flow regions of subcooled flow boiling. *ASME J. Heat Transf.* 120, 395–401.
- Kline, S.J., McClintock, F.A., 1953. Describing uncertainties in single-sample experiments. *Mech. Eng.* 75, 3–8.
- Liu, Z., Winterton, R.H.S., 1991. A general correlation for saturated and subcooled flow boiling in tubes and annuli, based on a nucleate pool boiling equation. *Int. J. Heat Mass Transf.* 34, 2759–2766.
- Owhaib, W., Palm, B., 2004. Experimental investigation of single-phase convective heat transfer in circular microchannels. *Exp. Therm. Fluid Sci.* 28, 105–110.
- Owhaib, W., Martín-Callizo, C., Palm, B., 2004. Evaporative heat transfer in vertical circular microchannels. *Appl. Therm. Eng.* 24, 1241–1253.
- Peng, X.F., Hu, H.Y., Wang, B.X., 1998. Boiling nucleation during liquid flow in microchannels. *Int. J. Heat Mass Transf.* 41, 101–106.
- Pethukov, B.S., Popov, V.N., 1963. Theoretical calculation of heat exchange in turbulent flow in tubes of an incompressible fluid with variable physical properties. *High Temp.* 1, 69–83.
- Prodanovic, V., Fraser, D., Salcudean, M., 2002. On the transition from partial to fully developed subcooled flow boiling. *Int. J. Heat Mass Transf.* 45, 4227–4738.
- Sato, T., Matsumura, H., 1964. On the conditions of incipient subcooled boiling with forced convection. *Bull. JSME* 7, 392–398.
- Shah, M., 1977. A general correlation for heat transfer during subcooled boiling in pipes and annuli. *ASHRAE Trans.* 83, 202–215.
- Tong, L.S., Tang, Y.S., 1997. *Boiling heat transfer and two-phase flow*, second ed. Taylor & Francis Publishers, 245–258.
- Yin, C.P., Yan, Y.Y., Lin, T.F., Yang, B.C., 2000. Subcooled flow boiling heat transfer of R-134a and bubble characteristics in horizontal annular duct. *Int. J. Heat Mass Transf.* 43, 1885–1896.